

Article

Improved Direct–Parallel Active Noise Control Systems for Narrowband Noise

Cheng-Yuan Chang , Ming-Han Ho and Sen M. Kuo

Department of Electrical Engineering, Chung Yuan Christian University, Taoyuan 320, Taiwan

* Correspondence: ccy@cycu.edu.tw

Abstract: Narrowband active noise control (NANC) systems are extensively used to cancel narrowband noise. Direct, parallel, and direct–parallel NANC systems use nonacoustic sensors to measure rotational speeds, and a bank of signal generators then produces synchronized sinusoidal waveforms as reference signals corresponding to the fundamental frequency of the undesired noise. The performance of direct NANC systems is based on the frequency difference between two adjacent reference input sinusoids. Parallel NANC systems apply several sinewave generators and two-weight adaptive filters in parallel to attenuate these narrowband components. Conventional direct–parallel NANC systems split these sinusoids into several mutually exclusive sets such that the distance between frequencies within sets is maximized. This paper proposes an improved direct–parallel NANC system in which reference sinusoidal signals are separated by amplitude to enhance efficiency and improve noise reduction performance. Several experiments were conducted using a muffler model to verify the performance of the proposed NANC system.

Keywords: direct–parallel form; active noise control; muffler; automobile noise

Academic Editors: Jian Kang,
Yangfan Liu and Woon-Seng Gan

Received: 3 October 2024

Revised: 16 December 2024

Accepted: 7 January 2025

Published: 13 January 2025

Citation: Chang, C.-Y.; Ho, M.-H.; Kuo, S.M. Improved Direct–Parallel Active Noise Control Systems for Narrowband Noise. *Acoustics* **2025**, *7*, 4. <https://doi.org/10.3390/acoustics7010004>

Copyright: © 2025 by the authors. Licensee MDPI, Basel, Switzerland. This article is an open access article distributed under the terms and conditions of the Creative Commons Attribution (CC BY) license (<https://creativecommons.org/licenses/by/4.0/>).

1. Introduction

Rotary machines, including motors and engines, are widely used in various applications, and they typically generate noise at their fundamental frequency and its harmonics, which are determined by their rotational speed [1–4]. In practice, 10 or more harmonics often contribute to undesired noise from machines. Furthermore, several types of industrial noise, such as those generated by compressors, fans, and propellers, are periodic. The mechanical motion of these noise sources can generally be observed directly by using an appropriate sensor. Such sensors can provide an electrical reference signal with the same fundamental frequency as the primary noise emitted. In addition, undesirable acoustic feedback in common active noise control (ANC) systems can be eliminated by using a nonacoustic sensor that is synchronized with the noise source. Such a sensor generates a reference signal that contains the fundamental frequency and all of the harmonics of the primary noise. Various techniques can be used to generate such a reference signal for an electronic ANC controller. These techniques are used to reduce periodic noise in many narrowband ANC (NANC) systems, including direct, parallel, and direct–parallel systems.

Glover [5] proposed a method for eliminating multiple sinusoidal or other periodic interferences. This method applies an adaptive filter to eliminate interferences and is effective in scenarios involving an auxiliary reference signal that contains the interference alone. In this method, the reference input is filtered such that it closely matches the interference noise and is then subtracted from the primary input. Another study [6] proposed an application based on Glover’s method for actively reducing narrowband noise.

In this application, a reference signal, which represents selected multiple-harmonic noise components, is generated from a predetermined table of values corresponding to a specified range of engine rotational speeds. If the reference signal includes all of the sinusoidal components of the interference, a notch filter for each sinusoid is created automatically by an NANC system. This notch filter tracks changes in frequency, thus providing a simple method for eliminating sinusoidal interference. However, if the frequencies of the reference sinusoids are similar, the filter length must be long enough to achieve sufficient resolution between adjacent frequencies [5]. Systems based on these principles are typically referred to as direct NANC systems and can eliminate multiple sinusoidal or periodic interferences.

A single-frequency component can be canceled by a simple two-weight adaptive filter. Thus, if undesired narrowband noise comprises M sinusoids, M two-weight adaptive filters can be connected in parallel to attenuate these narrowband components. This configuration is known as a parallel NANC system. Information in a synchronization signal is used to generate a set of reference sinusoids. Each sinusoid is used as the reference input for the corresponding channel of the two-weight adaptive filter. The main drawback of parallel NANC systems is their high computational complexity; they require applying multiple filters simultaneously, necessitating high hardware requirements such as additional processing units, memory, and sensors. They are thus both large and expensive. Accordingly, several recent studies have investigated miniaturizing and improving the efficiency of parallel NANC systems. For example, Zhu et al. [7] presented a system that removes dominant narrowband noise signals to improve computational efficiency. Another study [8] developed a computationally efficient parallel NANC system; however, this system can cancel only three target frequencies. Moreover, Zhang et al. [9] presented a parallel virtual sensing method for ANC feedback in a headrest, but this method can target only three undesirable narrowband frequencies.

NANC systems combining the aforementioned methods are direct-parallel systems. These systems combine multiple reference signal generators and their corresponding adaptive filters. A study [10] developed such a system to improve noise attenuation in automotive applications. This system separates a collection of many harmonically related sinusoids into mutually exclusive sets such that the distance between the frequencies within each set is maximized. If the number of reference signal generators is equal to the number of harmonics to be canceled, this system is equivalent to a parallel NANC system; each reference signal contains only one sinusoidal frequency corresponding to the narrowband noise [11].

In general, in a direct-parallel system for canceling M harmonics with K signal generators ($M > K$), each reference signal $x_k(n)$ ($k = 1, 2, \dots, K$) contains M/K staggered sinusoidal frequencies of every other k^{th} harmonic. Hence, the order of each adaptive filter can be reduced. This is because the frequency difference between any two successive sinusoidal components is larger than that in direct NANC systems.

In summary, direct NANC systems require long filters to eliminate noise with multiple harmonics; they are thus computationally expensive. Moreover, direct NANC systems have poor performance if the frequency separation between two consecutive harmonics is small. By contrast, parallel NANC systems reduce only one harmonic in each channel; they can thus have a short filter for each channel and a high learning rate. However, parallel NANC systems require multiple sinewave generators to produce reference sinusoids from the information provided by the corresponding synchronization signal, again resulting in high computational complexity and hardware costs.

A direct-parallel NANC system that separates a collection of several harmonically related sinusoids into mutually exclusive sets of maximally spaced frequencies could be more suitable for reducing narrowband noise in practice. Furthermore, this direct-

parallel architecture is scalable. Filters can be added as required to accommodate additional narrowband noise components. Thus, direct-parallel NANC systems constitute a versatile option for handling various noise sources with different frequency characteristics. Rotary machines produce narrowband noise at their fundamental frequency and its harmonics; typically, 10 or more frequencies must be canceled for such machines. Therefore, a direct-parallel NANC system is likely the most feasible solution for this problem.

This study proposes an improved direct-parallel NANC system for separating reference sinusoidal signals on the basis of the amplitudes of undesired tonal noise to improve noise reduction performance. The study used a mock-up of an automobile muffler to demonstrate the effectiveness of the proposed system. Experimental results show that the proposed method significantly improves the noise reduction performance when compared with conventional method. In the meantime, the improved algorithm will not result in higher computational effort than conventional method.

The rest of this paper is organized as follows. Section 2 presents conventional and improved direct-parallel NANC algorithms. Section 3 presents the setup and results of several real-time experiments conducted to demonstrate the effectiveness of the proposed system. The computational complexity of the improved direct-parallel form NANC system is also discussed. Finally, Sections 4 and 5 provides the discussions and conclusions.

2. Materials and Methods

Improved Direct-Parallel NANC System

Direct, parallel, and direct-parallel NANC systems are typically used to reduce narrowband noise. To produce a reference signal while avoiding the acoustic feedback problem, NANC systems capture a synchronous signal from the rotary machine instead of using a microphone; the captured signal is input to a bank of sine wave generators. Direct NANC systems use one sine wave generator and use the sum of multiple sinusoids as the reference input. If the frequencies of the reference sinusoids are similar, a long filter is required to achieve sufficient resolution between adjacent frequencies. Parallel NANC systems use a sinewave generator and a two-weight adaptive filter for each undesired tonal noise component, and these are connected in parallel to attenuate the components. Thus, such systems are expensive, particularly in scenarios that require canceling many noise frequencies. Direct-parallel NANC systems separate a collection of many harmonically related sinusoids into mutually exclusive sets of widely spaced frequencies. This approach of partitioning signal component frequencies can substantially improve the accuracy and rate of convergence of each adaptive filter.

Figure 1 presents an overview of a conventional direct-parallel NANC system, where $d(n)$ is narrowband noise containing M harmonics with frequencies f_1, f_2, \dots, f_M and n is the digital sample. Assume that the undesired noise comprises a total of 24 harmonic frequencies ($M = 24$) and the system has four signal generators ($K = 4$) for the reference input $x_k(n)$ ($k = 1, \dots, K$). Each reference input signal is the sum of M/K sinusoids with frequencies in $d(n)$. The staggered frequencies of each set for conventional direct-parallel NANC are outlined as follows:

$$\begin{aligned} k = 1 &\Rightarrow f_1, f_5, f_9, f_{13}, f_{17}, f_{21} \\ k = 2 &\Rightarrow f_2, f_6, f_{10}, f_{14}, f_{18}, f_{22} \\ k = 3 &\Rightarrow f_3, f_7, f_{11}, f_{15}, f_{19}, f_{23} \\ k = 4 &\Rightarrow f_4, f_8, f_{12}, f_{16}, f_{20}, f_{24} \end{aligned}$$

Therefore, the reference signal $x_k(n)$ is

$$x_k(n) = \sum_{l=1}^{M/K} A_{k,l} \sin(2\pi f_{k+4(l-1)}nT), \tag{1}$$

where $A_{k,l}$ is the amplitude of the l th sinusoid at frequency $f_{k+4(l-1)}$ and T is the sampling period. To improve the convergence speed of the error signal at the frequencies corresponding to the valleys of the magnitude response of $S(z)$, the amplitudes $A_{k,l}$ are

$$A_{k,l} = \frac{1}{|\hat{S}(e^{j(2\pi f_{k+4(l-1)})})|}, \tag{2}$$

for $k = 1, \dots, K$ and $l = 1, \dots, M/K$. Thus, the amplitude of the k^{th} reference sinusoid can be set as the inverse of the magnitude response of the secondary path at the corresponding frequency. Equation (2) is essentially similar to the normalized least mean square algorithm [12] that uses a global learning rate normalized by the power estimate of $x(n)$. In the proposed system, an equivalent learning rate is applied for each narrowband component.

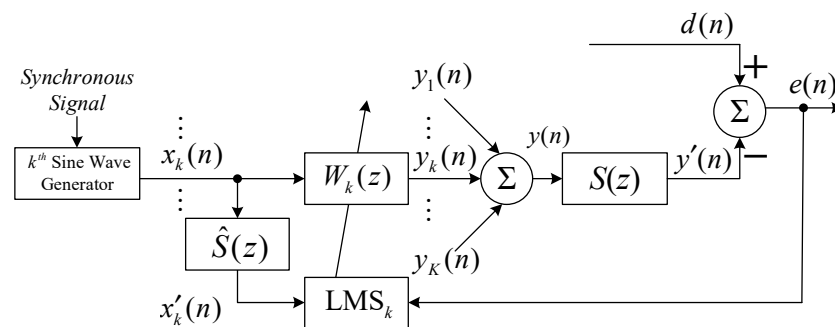


Figure 1. k^{th} channel of direct-parallel NANC system.

After each input signal is processed by its corresponding adaptive filter, the output signals are summed to obtain the antinoise signal $y'(n)$. The weight vector is then updated by the filtered-X least mean square (FXLMS) algorithm [13,14],

$$w_k(n + 1) = w_k(n) + \mu_k x'_k(n) e(n) \tag{3}$$

In Equation (3), $w_k(n) = [w_{0,k}(n), w_{1,k}(n), \dots, w_{N_k-1,k}(n)]^T$ is the weighting vector of $W_k(z)$, $x'_k(n) = [x'_k(n), x'_k(n - 1), \dots, x'_k(n - (N_k - 1))]^T$ is the filtered reference signal, and N_k is the filter length of the adaptive filter at the k^{th} channel. The parameter μ_k is the learning rate of the adaptive filter and satisfies the following constraint:

$$0 < \mu_k < \frac{2}{\lambda_{k,\max}} \tag{4}$$

where $\lambda_{k,\max}$ is the largest eigenvalue of the covariance matrix $R_k = E[x'_k(n)x_k'^T(n)]$ and $E[\cdot]$ is the expectation value. Assume that the estimated secondary path $\hat{S}(z)$ is equal to $S(z)$; hence, the filter length of $W_k(z)$ can be reduced, enabling an increase in the learning rate because the frequency difference between any two successive sinusoidal components in $x_k(n)$ is larger than that in a direct NANC system.

The objective of this study was to improve the active cancellation of automotive noise in direct-parallel NANC systems. In general, the power of automotive noise is mainly at lower frequency ranges, such as 100–700 Hz. Assume that $A_{k,l}$ represents the amplitude of

the l th harmonics of $x_k(n)$; hence, the learning rate μ_k for the corresponding adaptive filter $W_k(z)$ must satisfy the following stability constraint [13]:

$$\mu_k = \frac{1}{\max_l(A_{k,l})} \quad (5)$$

Consider, for example, the first set ($k = 1$). The learning rate must be small because the first few harmonics in each set usually have high amplitudes. Therefore, a conventional direct-parallel NANC system can only cancel the high-power harmonics in each set because of the small learning rate.

This study presents a novel method of determining the frequency components in each set of the direct-parallel NANC system. Consider, for example, a direct-parallel NANC system applied to 24 harmonic frequencies ($M = 24$) with 4 signal generators sets ($K = 4$); here, frequencies with similar amplitudes are grouped together, and frequencies in the same group are staggered among the sets. Assume that the frequency components f_1, f_2, \dots, f_{12} of the narrowband noise have similarly high amplitudes and that $f_{13}, f_{14}, \dots, f_{24}$ have similar but low amplitudes. Thus, the frequencies are grouped and staggered among the sets as follows:

$$\begin{aligned} k = 1 &\Rightarrow f_1, f_3, f_5, f_7, f_9, f_{11} \\ k = 2 &\Rightarrow f_2, f_4, f_6, f_8, f_{10}, f_{12} \\ k = 3 &\Rightarrow f_{13}, f_{15}, f_{17}, f_{19}, f_{21}, f_{23} \\ k = 4 &\Rightarrow f_{14}, f_{16}, f_{18}, f_{20}, f_{22}, f_{24}. \end{aligned}$$

Each set contains six staggered sinusoidal components with similar amplitudes. These reference signals are processed by their corresponding adaptive filters, and the output signals from each adaptive filter are then summed to obtain a canceling signal. Equation (5) indicates that the learning rates u_1 and u_2 are smaller than u_3 and u_4 because the frequencies in the first two sets have higher amplitudes than do those in the last two sets.

3. Results

3.1. Experimental Results

This study conducted experiments to determine the effectiveness of the proposed direct-parallel NANC system in handling narrowband noise from engines and motors. An electronic muffler was developed to reduce automotive noise at different rotational speeds, and the performance of the proposed system and that of a conventional NANC system were compared. The computational complexity of the system was also studied.

3.2. Experimental Setup

The electronic muffler used in the experiments is displayed in Figure 2a. This muffler was constructed from acrylic and had a width of 296 mm, height of 150 mm, and length of 450 mm; these are the same dimensions as those of the commercial automotive muffler (model number: #291545) from Jing-Tong Industrial (Chiayi, Taiwan; Figure 2b). Synthesized automotive noise was produced by a 6-in. primary speaker installed in a polyvinyl chloride tube to mimic an engine. A stainless-steel duct with a diameter of 5 cm served as the exhaust duct for the engine. Two 4-inches secondary speakers were installed in the acrylic electronic muffler. These speakers played an antinoise signal that destructively interfered with the undesired engine noise. Three “error microphones” were set at the open end of the electronic muffler to monitor the error (i.e., residual noise; Figure 2c). A digital signal processor (DSP; TMS320C6713 by Texas Instruments, Dallas, TX, USA) was used as the computing core, and a DSK6713IF-B interface card (HEG, Tokyo, Japan) was used for analog-to-digital (A/D) and digital-to-analog (D/A) data conversion. Power amplifiers

SA-98E (SMSL, Foshan, China) and preamplifiers MicTube Duo (ALESIS, Cumberland, MD, USA) were applied to amplify the signals for the speakers and microphones, respectively. Two low-pass filters with cutoff frequencies 750 Hz were used for antialiasing and smoothing the signals for A/D and D/A conversion. Because most automotive noise is below 700 Hz, the sampling frequency of the experiments was set to 2 kHz.

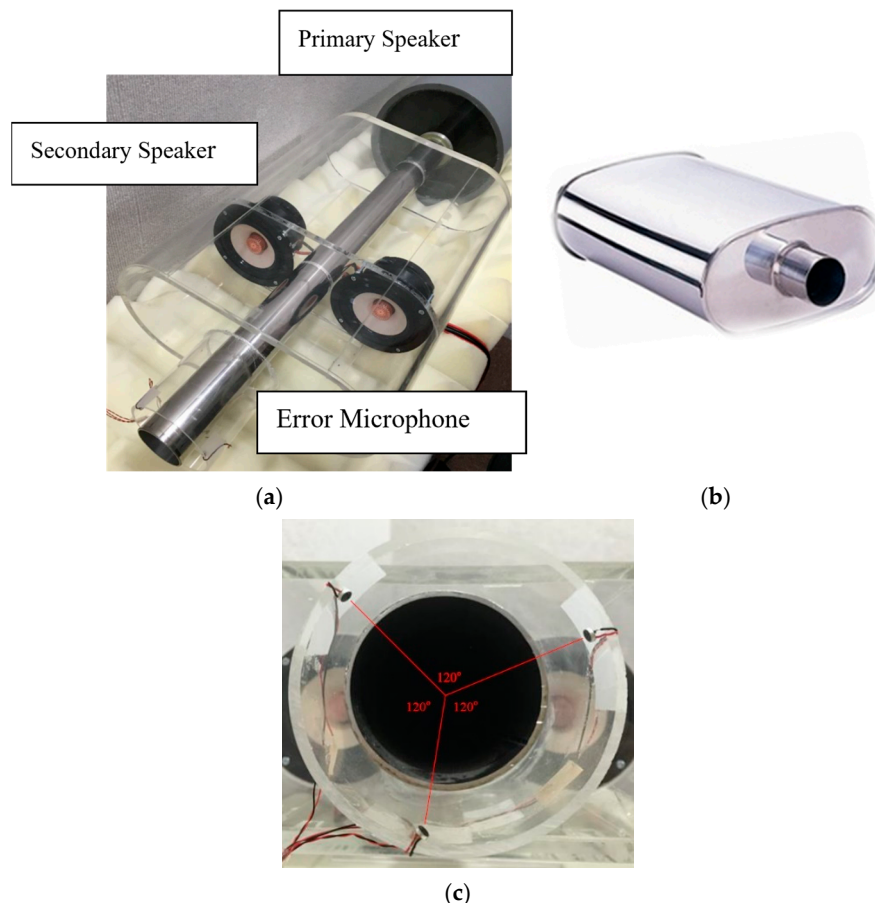


Figure 2. (a) Electronic muffler and (b) commercial muffler #291545. (c) Error microphones.

To minimize the error signal, an adaptive algorithm must accurately compensate for the secondary path. Accordingly, this study first tested the secondary path of the built electronic muffler by generating white noise from the DSP system. The secondary path included the transfer functions of the D/A converter, the smoothing filter, the power amplifier, information from the secondary speaker to the error microphone, the preamplifier, the antialiasing filter, and the A/D converter. Figure 3a illustrates a block diagram of the secondary path, and Figure 3b presents the magnitude response of the estimated secondary path $\hat{S}(z)$ with an acrylic muffler filter length L of 64. Clearly, the system's response was poor at frequencies below 100 Hz because the secondary speakers could not provide sufficient power. Moreover, its response at approximately 600 Hz was poor owing to the acoustic arrangement of the secondary speaker. If necessary, this poor response can be improved by changing the locations of the secondary speakers.

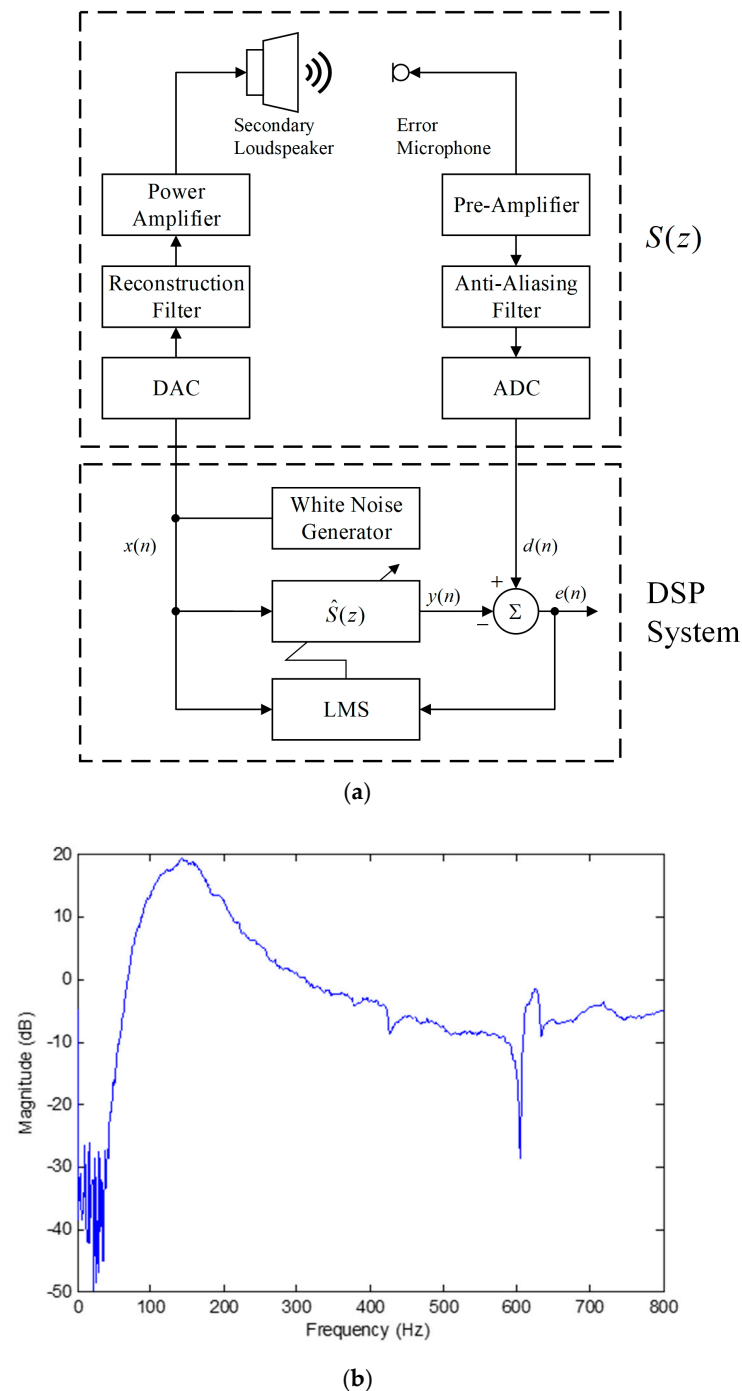


Figure 3. (a) Block diagram of the secondary path. (b) Magnitude response of the secondary path.

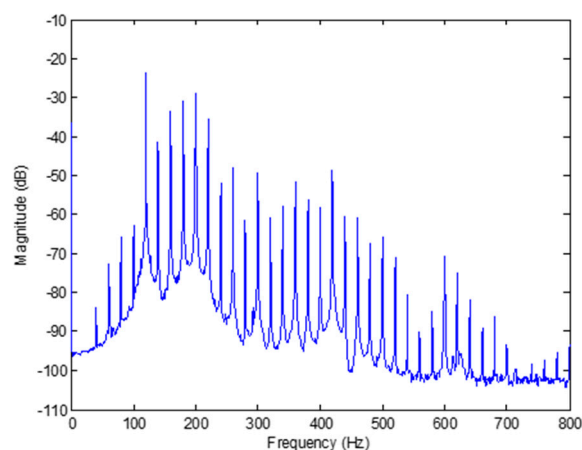
3.3. Waveform Synthesis and Experimental Results

The fundamental frequency for a four-stroke internal combustion engine of a vehicle is expressed as follows:

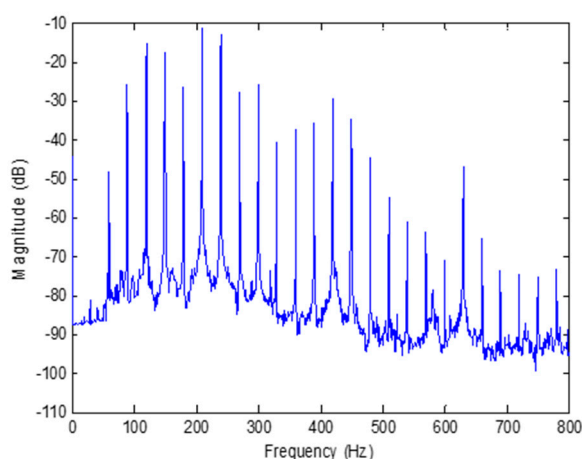
$$f_0 = \frac{N}{2} \cdot \frac{r}{60} \quad (6)$$

where N is the number of cylinders and r is the rotational speed [15]. Consider, for example, a four-cylinder automobile with a typical rotational speed of 2400 revolutions per minute (rpm); the fundamental frequency can be derived as $f_0 = \frac{4}{2} \cdot \frac{2400}{60} = 80$ Hz, and the separation between two consecutive harmonics can be derived as 20 Hz. For an automobile with a rotational speed of 3600 rpm, the fundamental frequency can be determined to be 120 Hz, and the separation between two consecutive harmonics can be

derived as 30 Hz. In this study, we used the primary speaker of the electronic muffler to generate a series of sinusoidal signals associated with white noise from 0 to 800 Hz to mimic engine noise [16]. The sounds received at the error microphones are illustrated in Figure 4; the main harmonics were determined to be between 100 and 700 Hz. The vertical axis of Figure 4 is a plot of the voltages of error microphones on a decibel scale. These results obtained before and after activating the proposed NANC systems were compared to evaluate their effectiveness.



(a)



(b)

Figure 4. Automobile engine noise, (a) 2400 rpm, (b) 3600 rpm.

In the first experiments, we tested the performance of the improved direct–parallel, direct and conventional direct–parallel NANC systems. The filter length for the estimated secondary path was 64. The sampling rate was 2 kHz, and the filter length for the direct NANC system was 650. The set number was $K = 7$ for the conventional and improved direct–parallel NANC systems. The staggered frequencies of each set for the conventional direct–parallel system are shown in Table 1. Because we aimed to reduce noise between 100 and 700 Hz, we selected four and three harmonics per set for noise associated with rotational speeds of 2400 and 3600 rpm, respectively. Table 2 presents the filter length and learning rate for each adaptive filter $W_k(z)$, $k = 1, \dots, 7$. The overall filter lengths for the seven sets were 2670 for the rotational speed of 2400 rpm and 2400 for the rotational speed of 3600 rpm.

Table 1. Staggered frequencies of each set of the conventional direct-parallel form NANC.

Sets	2400 rpm	3600 rpm
1	120, 260, 400, 540	90, 300, 510
2	140, 280, 420, 560	120, 330, 540
3	160, 300, 440, 580	150, 360, 570
4	180, 320, 460, 600	180, 390, 600
5	200, 340, 480, 620	210, 420, 630
6	220, 360, 500, 640	240, 450, 660
7	240, 380, 520, 660	270, 480

Table 2. Filter length/learning rate of the adaptive filter of each set for conventional direct-parallel NANC.

Sets	2400 rpm		3600 rpm	
	Filter Length	Learning Rate	Filter Length	Learning Rate
1	330	5×10^{-5}	500	10^{-4}
2	330	10^{-4}	300	8×10^{-5}
3	300	10^{-5}	300	3×10^{-5}
4	380	10^{-5}	300	5×10^{-5}
5	330	10^{-5}	300	5×10^{-5}
6	550	10^{-5}	300	5×10^{-4}
7	450	10^{-4}	400	10^{-4}

For the improved direct-parallel NANC system, the harmonics of noise associated with the rotational speed of 2400 rpm [Figure 4a] were divided into three groups according to amplitude (high, medium, and low). The high-amplitude frequencies were 120–220 Hz and were staggered in sets 1 and 2. The medium-amplitude frequencies were 240–460 Hz and were staggered in sets 3–5, and the remaining low-amplitude harmonics were staggered in sets 6 and 7. The harmonics of noise associated with the rotational speed of 3600 rpm were arranged similarly, as displayed in Figure 4b. Table 3 lists the frequencies in each set for the improved direct-parallel NANC system, and the filter length and learning rate for each set are presented in Table 4. The total filter lengths for the seven sets were 2370 and 2350 for noise associated with the rotational speeds of 2400 and 3600 rpm, respectively. The learning rates were selected through a trial-and-error method to maximize the value at convergence.

Table 3. Staggered frequencies of each set for improved direct-parallel NANC. Gray, Blue and Orange denote to high power, medium power and low power.

Sets	Power	2400 rpm	3600 rpm
1	High	120, 160, 200	90, 150, 210
2		140, 180, 220	120, 180, 240
3	Medium	240, 300, 360, 420	270, 330, 390
4		260, 320, 380, 440	300, 360, 420
5		280, 340, 400, 460	450, 540, 630
6	Low	480, 520, 560, 600, 640	480, 570, 660
7		500, 540, 580, 620, 660	510, 600

Table 4. Filter length/learning rate of the adaptive filter of each set for improved direct-parallel NANC. Gray, Blue and Orange denote to high power, medium power and low power.

Sets	Power	2400 rpm		3600 rpm	
		Filter Length	Learning Rate	Filter Length	Learning Rate
1	High	330	2×10^{-5}	350	3×10^{-5}
2		300	10^{-5}	350	10^{-5}
3	Medium	430	10^{-4}	350	7.5×10^{-4}
4		330	10^{-4}	350	8×10^{-4}
5		330	3×10^{-3}	300	3×10^{-3}
6	Low	350	3×10^{-3}	300	3×10^{-3}
7		300	10^{-3}	350	2×10^{-3}

Figure 5a presents the noise reduction rate at each frequency for noise associated with the rotational speed of 2400 rpm. Clearly, the direct and the conventional direct-parallel systems could effectively reduce high-amplitude harmonics at frequencies below 220 Hz by approximately 30 dB; however, these systems were less effective for lower-amplitude harmonics at frequencies above 300 Hz. By contrast, the proposed direct-parallel system reduced the harmonics by more than 20 dB at most frequencies above 300 Hz. Its poor performance at frequencies of 420 and 560–600 Hz could be attributed to the poor magnitude response of the secondary path. The average noise reduction rates observed at each harmonic frequency for the direct, conventional, and improved direct-parallel NANC systems were 10.4, 12.8, and 22.3 dB, respectively.

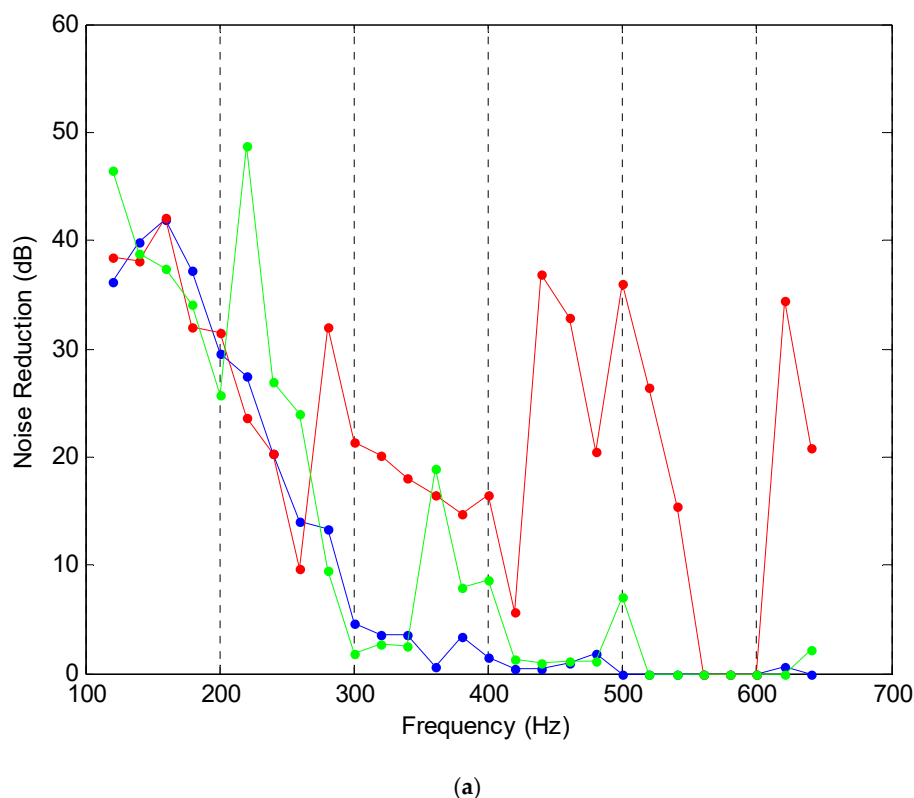
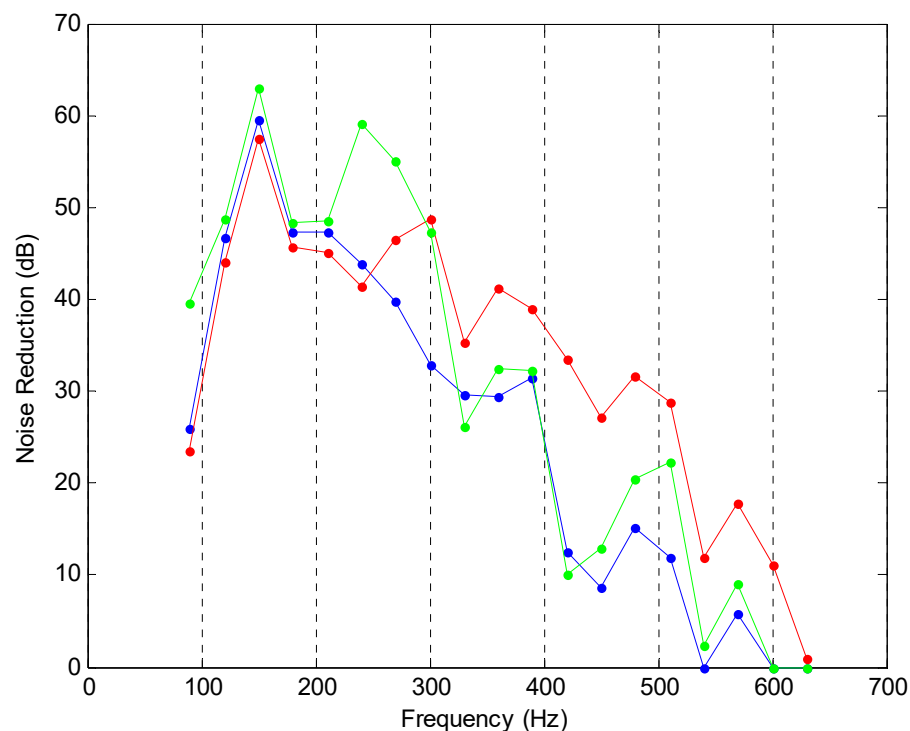


Figure 5. Cont.



(b)

Figure 5. Noise reduction in the direct (blue), conventional direct-parallel (green), and proposed direct-parallel (red) systems for (a) 2400- and (b) 3600-rpm noise.

Figure 5b displays plots of the performance of the systems for noise associated with the rotational speed of 3600 rpm. The improved direct-parallel NANC system clearly outperformed the other systems at frequencies above 300 Hz. The average noise reduction rates observed for the direct, conventional direct-parallel, and improved direct-parallel NANC systems were 25.6, 30.4, and 33 dB, respectively.

This study also investigated the effect of adding disturbances on the narrowband noise cancelation performance of the proposed direct-parallel system. The experimental setup is presented in Figure 6. An additional speaker was used to play a disturbance (2400-rpm noise) while the proposed system was activated to reduce 3600-rpm engine noise. This setup simulated the noise generated when another car passes by the noise-cancelled vehicle. Figure 7 illustrates plots of the performance results; the horizontal axis denotes the time in seconds, the vertical axis (left) denotes the frequency of the noise and the vertical axis at the right represents the color of the noise power. The proposed direct-parallel NANC system was started reducing the 3600-rpm engine noise at approximately 5 s, and the disturbance (2400-rpm engine noise) was added at approximately 10–12 s. Clearly, the proposed direct-parallel NANC system effectively reduced noise despite the disturbance.



Figure 6. Experimental setup for disturbance tests.

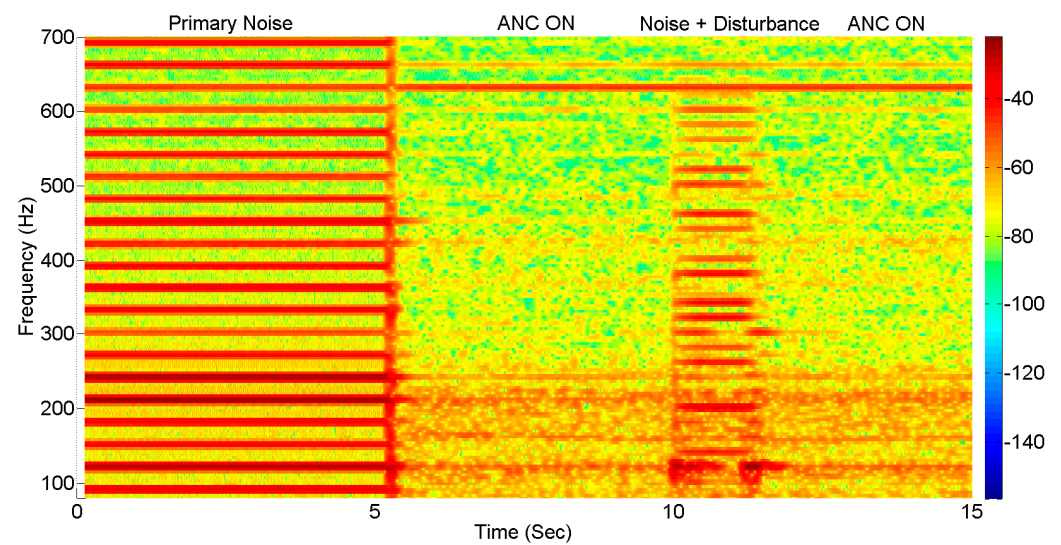


Figure 7. Performance of the proposed direct-parallel NANC system subjected to disturbance.

Finally, we compared the computational complexity of the conventional and proposed direct-parallel NANC systems. The filter length for the estimated secondary path is L ; thus, L multiplications and $L - 1$ additions are required to obtain $x'_k(n)$. The filter length for the adaptive filter in each set is N_k ; therefore, N_k multiplications and $N_k - 1$ additions are necessary to obtain $y_k(n)$. The FXLMS algorithm in Equation (3) costs two multiplications and one addition. The filter length of the adaptive filter is N_k , and it therefore requires $2N_k$ multiplications and N_k additions. Therefore, each sample requires $3N_k + L$ multiplications and $2N_k + L - 2$ additions. Obtaining the antinoise signal $y(n) = \sum_{k=1}^K y_k(n)$ requires $K - 1$ additions. Accordingly, the overall computational cost of obtaining the antinoise signal is presented in Table 5. The proposed system is not more computationally complex than the conventional system.

Table 5. Computational complexity of the conventional and proposed direct-parallel NANC systems.

Computational Complexity	2400 rpm		3600 rpm	
	Multiplications	Additions	Multiplications	Additions
Conventional	8458	5792	7648	5252
Proposed	7558	5192	7498	5152

4. Discussion

The proposed improved direct-parallel form NANC system can be extended to the multiple channel case using the developed algorithm. The advantage of the proposed

method over other NANC systems is that a similar computation requirement can be used to achieve better performance. This increases the feasibility for real-time applications. This aspect of the proposed algorithm is an improvement over the conventional direct-parallel NANC structures, which cancel only the harmonics with high amplitudes of the primary noise.

5. Conclusions

This study proposes an improved direct-parallel NANC system to enhance cancellation for signals in which the noise harmonics have substantially different amplitudes. Experimental results demonstrate that the proposed system better reduced narrowband noise. Moreover, it was robust to disturbances. Although the proposed system can control narrowband noise, it requires first measuring the power of each harmonic of the undesired noise before grouping harmonics with similar power by frequency. An automatic grouping mechanism could improve the practicality of the system for various applications.

Author Contributions: Conceptualization, C.-Y.C. and S.M.K.; methodology, C.-Y.C. and M.-H.H.; software, M.-H.H.; validation, C.-Y.C. and S.M.K.; writing—original draft preparation, C.-Y.C.; writing—review and editing, S.M.K.; supervision, S.M.K.; project administration, C.-Y.C. All authors have read and agreed to the published version of the manuscript.

Funding: This research received no external funding.

Data Availability Statement: The original contributions presented in the study are included in the article, further inquiries can be directed to the corresponding author.

Conflicts of Interest: The authors declare there are no conflicts of interest.

References

1. Abbink, V.; Landes, D.; Altinsoy, M.E. Experimental determination of the masking threshold for tonal powertrain noise in electric vehicles. *Acoustics* **2023**, *5*, 882–897. [[CrossRef](#)]
2. Liu, X.; Zheng, X.; Jia, Z.; Li, R.; Wan, B.; Liu, C.; Qiu, Y. A study on multi-channel active sound profiling algorithm for hybrid control of broadband and narrowband noise inside vehicles. *Measurement* **2024**, *237*, 115200. [[CrossRef](#)]
3. Chen, W.; Liu, Z.; Hu, L.; Li, X.; Sun, Y.; Cheng, C.; He, S.; Lu, C. A low-complexity multi-channel active noise control system using local secondary path estimation and clustered control strategy for vehicle interior engine noise. *Mech. Syst. Signal Process.* **2023**, *204*, 110786. [[CrossRef](#)]
4. Schubert, D.; Hecker, S.; Sentpali, S.; Buss, M. Feasibility analysis for active noise cancellation using the electrical power steering motor. *Acoustics* **2024**, *6*, 730–753. [[CrossRef](#)]
5. Glover, J.R., Jr. Adaptive noise cancelling applied to sinusoidal references. *IEEE Trans. Acoust. Speech Signal Process.* **1977**, *25*, 484–491. [[CrossRef](#)]
6. Pfaff, D.P.; Kapsokavathis, N.S.; Parks, N.A. Method for Actively Attenuating Engine Generated Noise. U.S. Patent 5,146,505, 8 September 1992.
7. Zhu, W.; Luo, L.; Xie, A.; Sun, J. A novel FELMS-based narrowband active noise control system and its convergence analysis. *Appl. Acoustics* **2019**, *156*, 229–245. [[CrossRef](#)]
8. Chen, W.; Lu, C.; Williams, H.; Liu, Z.; Sun, Y. Development and experimental verification of a new computationally efficient parallel narrowband active noise control system. *Appl. Acoustics* **2022**, *187*, 108510. [[CrossRef](#)]
9. Zhang, Z.; Wu, M.; Yin, L.; Gong, C.; Yang, J.; Cao, Y.; Yang, L. Robust parallel virtual sensing method for feedback active noise control in a headrest. *Mech. Syst. Signal Process.* **2022**, *178*, 109293. [[CrossRef](#)]
10. Yuan, Y.; Kapsokavathis, N.S.; Chen, K.; Kuo, S.M. Active Noise Control System. U.S. Patent 5,359,662, 25 October 1994.
11. Wang, H.; Sun, H.; Sun, Y.; Wu, M.; Yang, J. A narrowband active noise control system with a frequency estimation algorithm based on parallel adaptive notch filter. *Signal Process.* **2019**, *154*, 108–119. [[CrossRef](#)]
12. Wang, W.; Zhang, H. A new and effective nonparametric variable step-size normalized least-mean-square algorithm and its performance analysis. *Signal Process.* **2023**, *210*, 109060. [[CrossRef](#)]
13. Kuo, S.M.; Morgan, D.R. *Active Noise Control Systems*; Wiley: New York, NY, USA, 1996.
14. Widrow, B.; Stearns, S.D. *Adaptive Signal Processing*; Prentice-Hall: Englewood Cliffs, NJ, USA, 1985.

15. Chen, F.; Zhang, X. Synthesising the sound of a car engine based on envelope decomposition and overlap smoothing. *J. Vibroeng.* **2021**, *23*, 1254–1266. [[CrossRef](#)]
16. Ziegler, E.W.; Gardner, J.W. Active Sound Attenuation System for Engine Exhaust Systems and the Like. U.S. Patent 5,097,923, 24 March 1992.

Disclaimer/Publisher’s Note: The statements, opinions and data contained in all publications are solely those of the individual author(s) and contributor(s) and not of MDPI and/or the editor(s). MDPI and/or the editor(s) disclaim responsibility for any injury to people or property resulting from any ideas, methods, instructions or products referred to in the content.